

The pH dependence of the mechanism of reaction of hydrogen peroxide with a nonaggregating, non- μ -oxo dimer-forming iron(III) porphyrin in water

(peroxidase/cytochrome P-450/catalase/oxygen transfer)

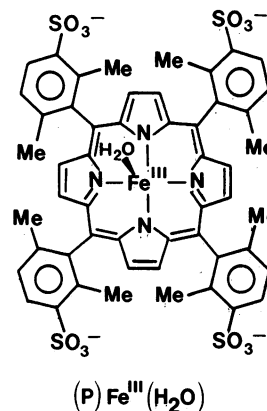
THOMAS C. BRUCE, MATTHIAS F. ZIPPLIES, AND WILLIAM A. LEE

Department of Chemistry, University of California, Santa Barbara, Santa Barbara, CA 93106

Contributed by Thomas C. Bruce, March 3, 1986

ABSTRACT The reaction of hydrogen peroxide with 5,10,15,20-tetrakis(2,6-dimethyl-3-sulfonatophenyl)porphinatoiron(III) hydrate [(P)Fe^{III}(H₂O)] has been investigated in water between pH 1 and pH 12. The water-soluble (P)Fe^{III}(H₂O) neither aggregates nor forms a μ -oxo dimer. The pH dependence and rate-limiting second-order rate constants (k_{12}) for oxygen transfer from H₂O₂ and HO₂⁻ to the iron(III) porphyrin were determined by trapping of the resultant higher-valent iron-oxo porphyrin species with 2,2'-azinodi(3-ethylbenzthiazoline)-6-sulfonate (ABTS). Reactions were monitored spectrophotometrically by following the appearance of the radical ABTS^{•+}. From a plot of the logarithm of the determined second-order rate constants for reaction of hydrogen peroxide with iron(III) porphyrin vs. pH, the composition of the transition states can be assigned for the three reactions that result in oxygen transfer to yield a higher-valent iron-oxo porphyrin species. The latter not only reacts with ABTS to provide ABTS^{•+} in a peroxidase-type reaction but also reacts with hydrogen peroxide to provide O₂ in a catalase-type reaction. The nitrogen base 2,4,6-collidine serves as a catalyst for oxygen transfer from hydrogen peroxide to the (P)Fe^{III}(H₂O) and (P)Fe^{III}(HO) species. The preferred mechanism involves a 1,2-proton shift concerted with heterolytic cleavage of the peroxide O—O bond. An analogous mechanism is believed to occur in the peroxidase enzymes.

A knowledge of the mechanism of reaction of hydrogen peroxide with iron(III) porphyrins is germane to our understanding of the mechanisms of the peroxidase (1) and catalase (2) enzymes and the peroxide shunt reaction of the cytochrome P-450 enzymes (3-10). Though the reaction of hydrogen peroxide with various iron(III) porphyrins in H₂O has received considerable attention, we find that much of the past work (11-23) is both incomplete and obscured by the occurrence of metalloporphyrin destruction, aggregation in water, and dimerization in basic media. These difficulties have prevented investigators from carrying out a thorough pH dependence study on this biologically relevant reaction. To accomplish such a study it is necessary that the iron(III) porphyrin be water soluble, nonaggregating, and sterically blocked to prevent μ -oxo dimer formation. In addition, the higher-valent iron-oxo porphyrin species formed upon oxygen transfer from hydrogen peroxide to iron(III) porphyrin should be trapped by a suitable substrate to prevent its degradation. These requirements have been completely met by utilizing 5,10,15,20-tetrakis(2,6-dimethyl-3-sulfonatophenyl)porphinatoiron(III) hydrate [(P)Fe^{III}(H₂O)]



as the iron(III) porphyrin and 2,2'-azinodi(3-ethylbenzthiazoline)-6-sulfonate (ABTS) as trapping reagent.

METHODS AND MATERIALS

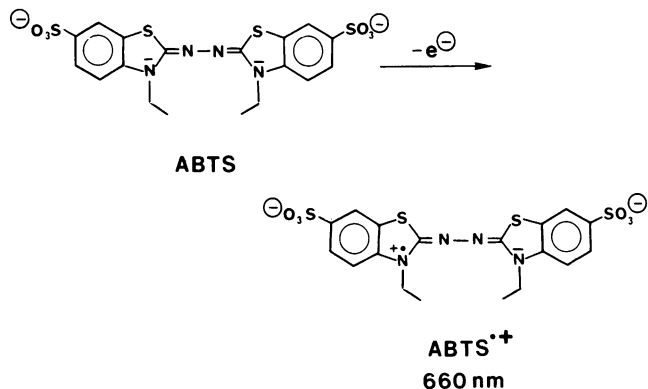
(P)Fe^{III}(H₂O) has been synthesized and characterized elsewhere (24). The diammonium salt of ABTS was obtained from Sigma. 2,4,6-Collidine was purchased from Aldrich and shown to be 99.9% pure by gas chromatography. All buffer and salt solutions were extracted with 0.01% dithizone in carbon tetrachloride (below pH 7) or passed over a column of Chelex 100 (Bio-Rad) to remove any heavy metal contamination. The cuvettes were regularly soaked in 1% EDTA overnight and washed extensively with doubly distilled water. The concentration of hydrogen peroxide (Mallinckrodt 30%) was determined iodometrically. Oxygen evolution was measured with a Yellow Springs Instrument model 53 oxygen monitor (5331 oxygen electrode), and reactions were followed spectrophotometrically with a Perkin-Elmer 553 rapid-scan spectrophotometer or a Durrum stopped-flow spectrophotometer interfaced to a North Star computer equipped with OLIS 3820 data acquisition and processing software (On-Line Instruments Systems, Jefferson, GA).

Kinetic Studies. All reactions were carried out in aqueous solutions at 30°C and ionic strength μ of 0.21 M (with NaNO₃) with [H₂O₂] \gg [(P)Fe^{III}(H₂O)] = 0.4-5 μ M. In practice the concentration of ABTS was 50- to 70-fold in excess over that of H₂O₂. The following buffers and concentrations were used: ClCH₂COOH/ClCH₂COO⁻ (pH 2.73, [total buffer, B_T] = 10-100 mM), CH₃COOH/CH₃COO⁻ (pH 3.95 to 5.2, [B_T] =

10–100 mM), 2,4,6-collidine·HCl/2,4,6-collidine (pH 6.18 to 8.64, [B_T] = 4–60 mM), H₂PO₄⁻/HPO₄²⁻ (pH 8.00, [B_T] = 2–50 mM), HCO₃⁻/CO₃²⁻ (pH 9.28 and 9.85, [B_T] = 8–80 mM). Below pH 2.7 the acidity was maintained with HCl and above pH 10 it was maintained with KOH.

RESULTS AND DISCUSSION

Under the conditions of constant pH and [ABTS] >> [hydrogen peroxide] >> [(P)Fe^{III}(H₂O)] the pseudo-first-order rate constants (*k*_{obs}) for the formation (660 nm) of ABTS^{•+} were found to be independent of the initial concentrations of



ABTS and hydrogen peroxide and to be linearly dependent upon the concentration of added (P)Fe^{III}(H₂O). The initial rates (*k*_i) were found to be linearly dependent upon the concentrations of added hydrogen peroxide and (P)Fe^{III}(H₂O) but independent of the concentration of ABTS. These results establish that (i) the iron(III) porphyrin catalyst is not saturated with hydrogen peroxide; (ii) the rate-determining step is the reaction of hydrogen peroxide with iron(III) porphyrin; and (iii) ABTS is oxidized to its radical ABTS^{•+} in a rapid reaction that follows the rate-determining step. Plots of *k*_{obs} vs. total buffer concentrations at constant values of pH (pH 2.73 to 9.85)—with chloroacetate, acetate, phosphate, and carbonate buffers—were found to provide zero or very slight positive or negative slopes. This result shows that these buffers do not catalyze the reaction. Dividing the values of *k*_{obs} at zero buffer concentration by the concentration of added iron(III) porphyrin provides the pH-dependent second-order rate constants *k*_{iy}. Fig. 1 is a plot of log *k*_{iy} vs. pH. Inspection of the figure shows that at low, intermediate, and

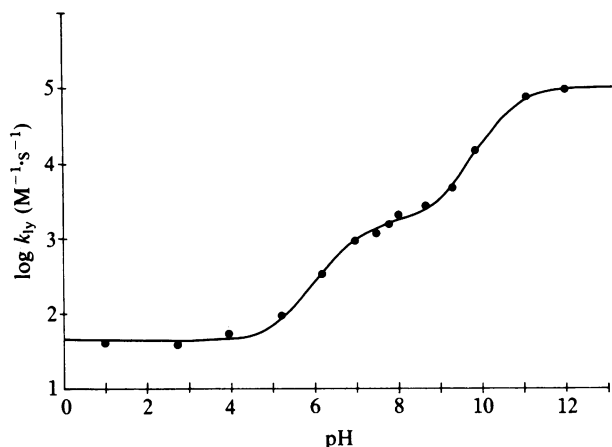
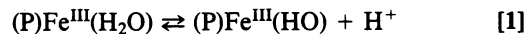


Fig. 1. Plot of the log of the rate constants for non-buffer-catalyzed (*k*_{iy}) reaction of (P)Fe^{III}(H₂O) with hydrogen peroxide vs. pH (30°C, μ = 0.21 M).

high pH there exist plateaus at which the rate constant *k*_{iy} is independent of pH. The ascending portion of the curve that connects the plateaus at low and intermediate pH reflect the pK_a of (P)Fe^{III}(H₂O), which was determined independently by spectrophotometric titration (393 and 413 nm) as 7.25 (Eq. 1), while the ascending curve



connecting the intermediate plateau and the plateau at high pH pertains to the pK_a of H₂O₂. The pH–log *k*_{iy} profile of Fig. 1 defines the composition of the iron(III) porphyrin–hydroperoxide complexes involved in the three competing reactions for hydroperoxide oxidation of the iron(III) porphyrin. The compositions of these complexes are (P)Fe^{III}(H₂O)(H₂O₂) at low pH, (P)Fe^{III}(HO)(H₂O₂) at intermediate pH, and (P)Fe^{III}(OH)(HO₂) at high pH. A homolytic peroxide O–O bond cleavage in intermediates would provide HO· plus iron(IV)-oxo porphyrin, while a heterolytic O=O bond cleavage would result in the formation of iron(IV)-oxo porphyrin π-cation radical and H₂O. The products of either reaction type would be rapidly trapped by ABTS, and at high pH hydrogen peroxide can also act as a trap. At low pH ABTS^{•+} is formed in 100% yield; as the pH increases, the yield decreases to 20% while the percent yield of O₂ increases.

A number of kinetically equivalent structures may be drawn for the transition states associated with the reactions at low, intermediate, and high pH, TS₁, TS₂, and TS₃, respectively. The kinetically equivalent structures differ by the position of a proton. Possible structures are shown in Fig. 2. The structure TS₁B represents general-acid catalysis and

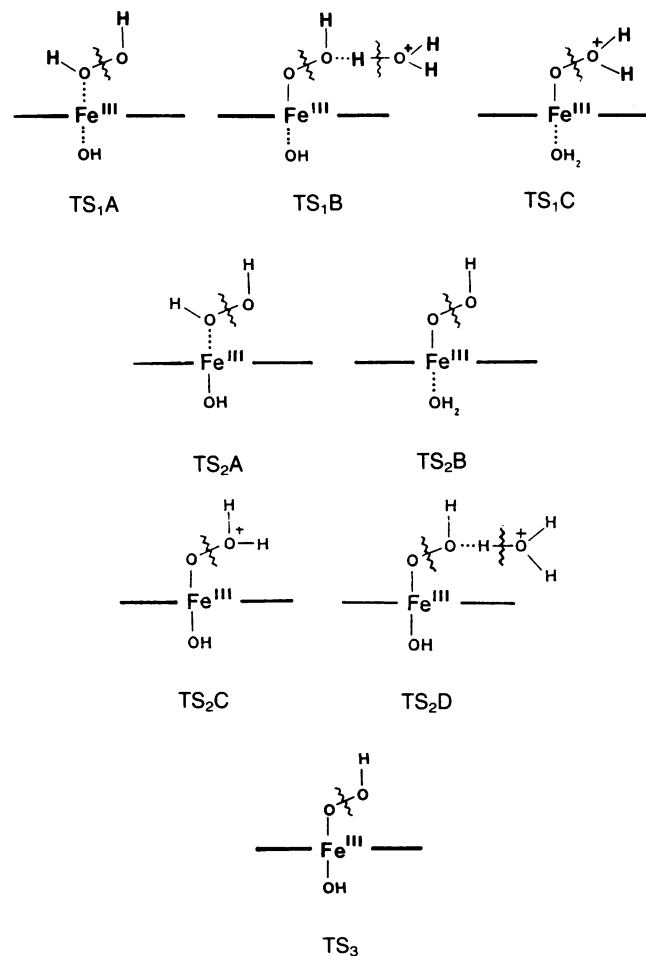
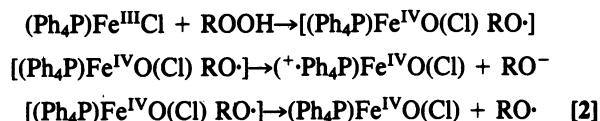


Fig. 2. Possible structures of transition states.

TS₁C represents specific acid catalysis by H₃O⁺. Structure TS₁B is considered highly unlikely on the basis of the inability to detect general catalysis by ClCH₂CO₂H/GlCH₂CO₂⁻ and CH₃CO₂H/CH₃CO₂⁻ buffers at lower pH values. The inability to observe such catalysis is not due to ligation of the carboxylate species to the iron(III) porphyrin. Binding studies showed no evidence for carboxylate ligation for (P)Fe^{III} (H₂O). Among the TS₂ structures, TS₂D may be discounted on the basis that the observed rate constant would require ligation of the HOO⁻ moiety with an equilibrium constant of about 10⁷ M⁻¹, which is unlikely since iron(III) porphyrins do not strongly ligate two highly basic oxyanions. Thus, spectrophotometric titration of (P)Fe^{III}(HO) to pH 14 shows no evidence for ligation of a second HO⁻ species, and likewise the addition of CH₃O⁻ to a dichloromethane solution of (P)Fe^{III}(CH₃O) does not result in the dimethoxy species, (P)Fe^{III}(CH₃O)₂. The structure TS₂B should be somewhat more stable than TS₂A on the basis of the base strengths anticipated for the ligated oxygens of HO⁻ and HOO⁻. In summary, at low pH the transition state structure is most likely represented by TS₁A or TS₁C, while at intermediate pH values TS₂A, TS₂B, and TS₂C are the likely candidates, and at high pH the transition state structure can be represented only by TS₃.

For the transition state structures TS₁C and TS₂C the leaving group must be H₂O and therefore O—O bond scission would be heterolytic. With the transition state structures TS₁A, TS₂A, TS₂B, and TS₃ the leaving group can be either HO· or HO⁻, dependent upon whether the O—O bond scission is homolytic or heterolytic. We have previously presented evidence (25) in favor of rate-determining homolytic bond scission for the reaction of 5,10,15,20-tetrakis(phenyl)porphyrinatoiron(III) chloride with alkyl peroxides and hydrogen peroxide in methanol (Eq. 2). In Eq. 2 the species (⁺Ph₄P)Fe^{IV}O(Cl) represents the chloride salt of the iron(IV)-oxo tetraphenylporphyrin π-cation radical.



Though ClCH₂COOH/ClCH₂COO⁻, CH₃COOH/CH₃COO⁻, H₂PO₄⁻/HPO₄²⁻, and HCO₃⁻/CO₃²⁻ buffers did not exhibit catalysis of the reaction of hydrogen peroxide and the iron(III) porphyrin species, marked catalysis was seen in the presence of 2,4,6-collidine·H⁺/2,4,6-collidine buffer in the pH range of the intermediate plateau. Sample buffer dilution plots are shown in Fig. 3. From the slopes of such plots there may be calculated the third-order rate constants ($k_{\text{BH}} = 2.0 \times 10^4 \text{ M}^{-2}\text{s}^{-1}$, $k_{\text{B}} = 8.2 \times 10^4 \text{ M}^{-2}\text{s}^{-1}$) for the reactions involving H₂O₂ + (P)Fe^{III}(HO) + 2,4,6-collidine·H⁺ and H₂O₂ + (P)Fe^{III}(HO) + 2,4,6-collidine, respectively. The finding that the collidine buffer exhibits catalysis whereas the other buffers do not is unusual. If the collidine buffer catalysis is attributed to general-acid and general-base catalysis, then catalysis by both oxygen acid and base buffers would be expected. The rate constants for general-acid and general-base catalyzed proton transfer from oxygen are primarily dependent on the proton basicity of the buffer base and secondarily on electrostatic effects (26–29) in the transition state which are related to the nature of the basic atom

(i.e., —O⁻ vs. —N:). Further studies with other oxygen- and nitrogen-centered buffer pairs are required to clarify this aspect of the study.

As in the case of the structures depicting the transition states for the noncatalyzed reaction of hydroperoxide and iron(III) porphyrin at low, intermediate, and high pH, a

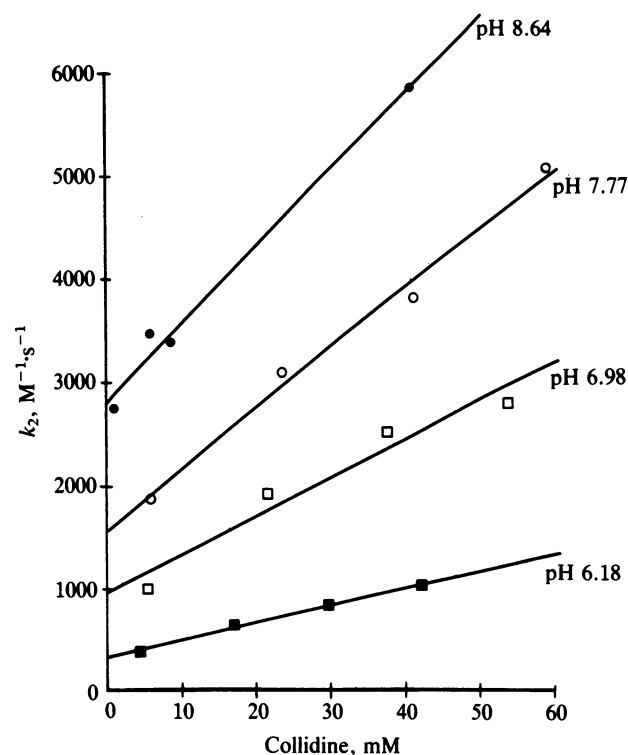
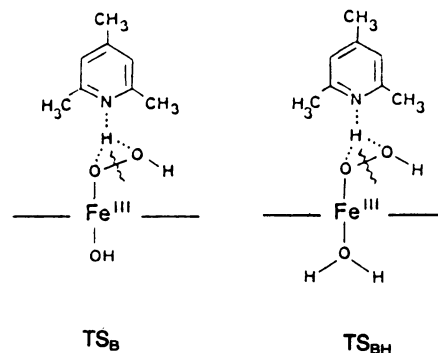


FIG. 3. Change in second-order rate constants (k_2) with change in the concentration of total collidine at different pH values. Every k_2 value is derived from a plot of the observed pseudo-first-order rate constant (k_{obs}) vs. [(P)Fe^{III}(H₂O)].

number of structures may be considered for the transition states of both the 2,4,6-collidine·H⁺ and 2,4,6-collidine free-base catalysis. These differ by the position of a proton, and their kinetic competence can be judged by a knowledge of the various acid–base equilibrium constants. Structure TS_B below represents a competent structure for 2,4,6-collidine general-base catalysis. The stoichiometry of the transition state for the 2,4,6-collidine·H⁺-catalyzed reaction is [2,4,6-collidine·H⁺] + [(P)Fe^{III}(HO)(H₂O₂)]. Since the pK_a values of 2,4,6-collidine·H⁺ and (P)Fe^{III}(H₂O) are almost identical (7.48 vs. 7.25), there is little thermodynamic barrier to free transfer of the buffer acid proton to (P)Fe^{III}(HO) to provide 2,4,6-collidine + (P)Fe^{III}(H₂O). This consideration establishes TS_{BH}⁺ as a competent transition state structure for 2,4,6-collidine·H⁺ buffer catalysis. The mechanisms associated with TS_B and TS_{BH} are general-base-catalyzed 1,2-proton shifts with concerted O—O bond cleavage.



Since H₂O is the leaving group, the mechanism of O—O bond cleavage is required to be heterolytic. Structures TS_B and TS_{BH} are both kinetically plausible transition states and we suggest them as models for the distal base catalysis proposed in the peroxidase enzymes.

This study was supported by grants from the National Institutes of Health and the National Science Foundation. M.F.Z. expresses appreciation to BASF of the Federal Republic of Germany for a postdoctoral fellowship.

1. Dunford, H. B. & Stillman, J. S. (1976) *Coord. Chem. Rev.* **19**, 187-251.
2. Schonbaum, G. R. & Chance, B. (1976) in *The Enzymes*, ed. Boyer, P. D. (Academic, New York), 3rd Ed., Vol. 13, pp. 363-408.
3. Hrycay, E. G. & O'Brien, P. J. (1971) *Arch. Biochem. Biophys.* **147**, 14-27.
4. Hrycay, E. G. & O'Brien, P. J. (1973) *Arch. Biochem. Biophys.* **157**, 7-22.
5. Kladlubar, K. C., Morton, K. C. & Ziegler, D. M. (1973) *Biochem. Biophys. Res. Commun.* **54**, 1255-1261.
6. Hrycay, E. G. & O'Brien, P. J. (1974) *Arch. Biochem. Biophys.* **160**, 230-245.
7. Nordblom, G. D., White, R. E. & Coon, M. J. (1976) *Arch. Biochem. Biophys.* **175**, 524-533.
8. Blake, R. C. & Coon, M. J. (1981) *J. Biol. Chem.* **256**, 12127-12133.
9. McCarthy, M. B. & White, R. E. (1983) *J. Biol. Chem.* **258**, 9135-9158.
10. Estabrook, R. W., Martin-Wixtrom, C., Saeki, Y., Rennenburg, R., Hildebrandt, A. & Werringloer, J. (1984) *Xenobiotica* **14**, 87-104.
11. von Euler, H. & Josephson, K. J. (1927) *Justus Liebigs Ann. Chem.* **456**, 111.
12. Kremer, M. L. (1965) *Trans. Faraday Soc.* **61**, 1453-1458.
13. Kremer, M. L. (1967) *Trans. Faraday Soc.* **63**, 1208-1214.
14. Gatt, R. & Kremer, M. L. (1968) *Trans. Faraday Soc.* **64**, 721-726.
15. Brown, S. B., Dean, T. C. & Jones, P. (1970) *Biochem. J.* **117**, 741-744.
16. Portsmouth, D. & Beal, E. A. (1971) *Eur. J. Biochem.* **19**, 479-487.
17. Jones, P., Robson, T. & Brown, S. B. (1973) *Biochem. J.* **135**, 353-365.
18. Jones, P., Prudhoe, K., Robson, T. & Kelly, H. C. (1974) *Biochemistry* **13**, 4279-4284.
19. Kelly, H. C., Davies, D. M., King, M. J. & Jones, P. (1977) *Biochemistry* **16**, 3543-3549.
20. Jones, P., Mantle, D., Davies, D. M. & Kelley, H. C. (1971) *Biochemistry* **16**, 3974-3978.
21. Hatzikonstantinou, H. & Brown, S. B. (1978) *Biochem. J.* **174**, 893-900.
22. Jones, P., Mantle, D. & Wilson, I. (1983) *J. Chem. Soc. Dalton Trans.*, 161-164.
23. Traylor, T. G., Lee, W. A. & Stynes, D. V. (1984) *J. Am. Chem. Soc.* **106**, 755-764.
24. Zippies, M. F., Lee, W. A. & Bruice, T. C. (1986) *J. Am. Chem. Soc.*, in press.
25. Lee, W. A. & Bruice, T. C. (1985) *J. Am. Chem. Soc.* **107**, 513-514.
26. Bruice, P. Y. (1984) *J. Am. Chem. Soc.* **106**, 5959-5964.
27. Kresge, A. J., Chen, H. L., Chiang, Y., Murrill, E., Payne, M. A. & Sagatys, D. S. (1971) *J. Am. Chem. Soc.* **93**, 413-423.
28. Kresge, A. J. & Chiang, Y. (1983) *J. Am. Chem. Soc.* **95**, 803.
29. Ewing, S. P., Lockshon, D. & Jencks, W. P. (1980) *J. Am. Chem. Soc.* **102**, 3072-3084.